Journal of Alloys and Compounds 500 (2010) 22–25

Contents lists available at ScienceDirect

Journal of Alloys and Compounds

journal homepage: www.elsevier.com/locate/jallcom

High thermoelectric performance of reduced lanthanide molybdenum oxides densified by spark plasma sintering

Jianxiao Xu[a,*], Monica Sonne[a], Shun-ichi Yanangiya[a], Ngo Van Nong[a], Nini Pryds[a,*], Mats Nygren[b], Holger Kleinke[c]

[a] Fuel Cells and Solid State Chemistry Division, Risø National Laboratory for Sustainable Energy, Technical University of Denmark, 4000 Roskilde, Denmark
[b] Department of Inorganic Chemistry, Arrhenius Laboratory, Stockholm University, SE-10691 Stockholm, Sweden
[c] Department of Chemistry, University of Waterloo, Waterloo, Ontario, Canada N2L 3G1

ARTICLE INFO

Article history:
Received 11 March 2010
Received in revised form 22 March 2010
Accepted 23 March 2010
Available online 1 April 2010

Keywords:
Thermoelectric
Molybdenum oxides
Power factor
Thermal conductivity
Spark plasma sintering

ABSTRACT

Four highly reduced molybdenum oxides $LnMo_8O_{14}$ (Ln = La, Ce, Nd and Sm) containing bicapped Mo_8 clusters were synthesized via solid state reaction followed by spark plasma sintering. The thermoelectric properties were investigated, and $NdMo_8O_{14}$ exhibits the best performance with the maximum power factor of 177 $\mu W/mK^2$ at 1000 K. The highest ZT of $NdMo_8O_{14}$ was determined to be around 0.1 at 1000 K.

1. Introduction

The performances of thermoelectrics can be defined by the dimensionless figure of merit ZT [1], where $ZT = T \times (S^2\sigma)/\kappa$ (T is the absolute temperature, S is the Seebeck coefficient, σ is the electrical conductivity and κ is the total thermal conductivity). High-performance thermoelectric materials must have a large Seebeck coefficient, high electrical conductivity but low thermal conductivity in order to achieve a high ZT value. Since the discovery of unexpectedly good thermoelectric properties of p-type $NaCo_2O_4$ [2], intensive research has been devoted to discover new oxide materials [3–12] due to their natural advantages, e.g. good thermal stability, low cost, and environmental friendliness. Several thermoelectric modules [13–15] made with oxides have been developed, while the thermoelectric properties of n-type oxides still need to be improved. Recently, dually doped $Zn_{0.96}Al_{0.02}Ga_{0.02}O$ [16] was reported to show excellent thermoelectric performance with ZT = 0.65 at 1247 K, which was the highest ZT values so far for bulk n-type oxides. We commenced a study on n-type molybdenum oxides containing Mo clusters for thermoelectric heat recovery application because of their semiconducting behaviors and large thermopower [17]. Moreover, the structures of molybdenum oxides are rather complex [18–23], which could contribute to a low thermal conductivity.

Spark Plasma Sintering (SPS) technique is a unique sintering method combining mechanical pressure and an electric energy in a pulse shape as the heat source for sintering [24]. Nowadays, SPS has been developed and commonly used to prepare and densify various materials for thermoelectric research [8,25–30]. One of the main advantages of the SPS technique has been demonstrated to be the rapid densification of various materials in a very short time with respect to the conventional sintering method and hot pressing. In this study, we report the enhanced thermoelectric properties of lanthanide molybdenum oxides by spark plasma sintering.

2. Experimental

Four lanthanide molybdenum oxides $LaMo_8O_{14}$, $CeMo_8O_{14}$, $NdMo_8O_{14}$, and $SmMo_8O_{14}$ have been prepared from stoichiometric mixtures of Ln_2O_3 (Ln = La, Ce, Nd, and Sm), Mo and MoO_3 by conventional solid state reaction. The details can be found elsewhere [17].

Before SPS processing, the powders were ball-milled with ethanol for 24 h in order to achieve a smaller particle size of ca. 2 μm. The final processing was carried out using the spark plasma sintering system (Dr. Sinter SPS 2050, Sumitomo Coal Mining Co., Ltd., Japan). The pulsed electric current was passed through the sample under vacuum (10^{-3} bar,) while a uniaxial pressure of 50 MPa was applied. The powders were loaded in cylindrical graphite dies with an inner diameter of 0.5 in. and heated to the final sintering temperature using a heating rate of 100 K/min. In the temperature range $T < 1273$ K, the temperature was measured and regulated by a thermocouple, which was inserted into the die; while for $T \geq 1273$ K, the temperature was measured and regulated by an optical pyrometer focused on the surface of

* Corresponding authors.
E-mail addresses: jiax@risoe.dtu.dk (J. Xu), nipr@risoe.dtu.dk (N. Pryds).

0925-8388/$ – see front matter © 2010 Elsevier B.V. All rights reserved.
doi:10.1016/j.jallcom.2010.03.201

the die. During the experiments, there is no significant displacement or shrinkage of sample until the sintering temperature reaches 1573 K, where binary molybdenum oxides start to decompose also. In the final processing, a lower sintering temperature of 1473 K and higher uniaxial pressure of 110 MPa were used in order to ensure the full densification while avoiding decomposing of the powder. The pellets obtained after the SPS processing were polished to remove the graphite foil. The densities for all pellets were measured using Archimedes method to be around 75% of theoretical values.

3. Characterization

X-ray powder diffraction patterns were collected at ambient temperature from 5° to 80° with a step of 0.02° on a Bruker D8 diffractometer with Cu Kα radiation.

Electric transport properties of four compounds were measured on bar shaped pellets with approximate dimension of 3 mm × 3 mm × 8 mm using ZEM3-M10 unit from ULVAC Technologies, Inc. Japan. Electrical conductivity and Seebeck coefficient measurements were carried out simultaneously from room temperature to 1152 K under vacuum. The thermal conductivity of $NdMo_8O_{14}$ was determined from the density (d), thermal diffusivity (α), and specific heat (C_p) via the equation: $\kappa = d \times \alpha \times C_p$. The thermal diffusivity of the pellet (12.7 mm diameter × 3 mm thickness) were measured by Netzsch LFA-457 laser flash apparatus under N_2 flow between room temperature and 1164 K with a heating rate of 5 K/min. The specific heat was determined by the ratio method comparing with the reference sample, inconel, during the thermal diffusivity measurement.

4. Results and discussion

Fig. 1 presents the XRD patterns of all samples prepared by conventional solid state reaction. The sintering procedure was optimized and all samples were examined to be pure phases according to the International Crystal Structure Database (ICSD).

The temperature dependence of the electrical conductivity for $LnMo_8O_{14}$ (Ln = La, Ce, Nd, Sm) densified by spark plasma sintering are shown in Fig. 2. With increasing temperature, the electrical conductivity of all the samples increases, indicating semiconducting behavior. The electrical conductivity at room temperature was measured to be 120 Ω^{-1} cm^{-1} for $LaMo_8O_{14}$, 532 Ω^{-1} cm^{-1} for $CeMo_8O_{14}$, 303 Ω^{-1} cm^{-1} for $NdMo_8O_{14}$, and 340 Ω^{-1} cm^{-1} for $SmMo_8O_{14}$, which are significantly higher than the samples by den-

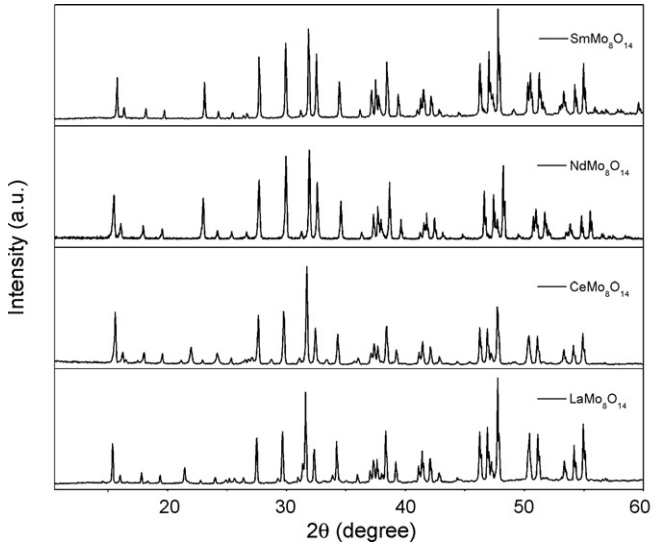

Fig. 1. XRD patterns of $LaMo_8O_{14}$, $CeMo_8O_{14}$, $NdMo_8O_{14}$ and $SmMo_8O_{14}$ prepared by conventional solid state reactions.

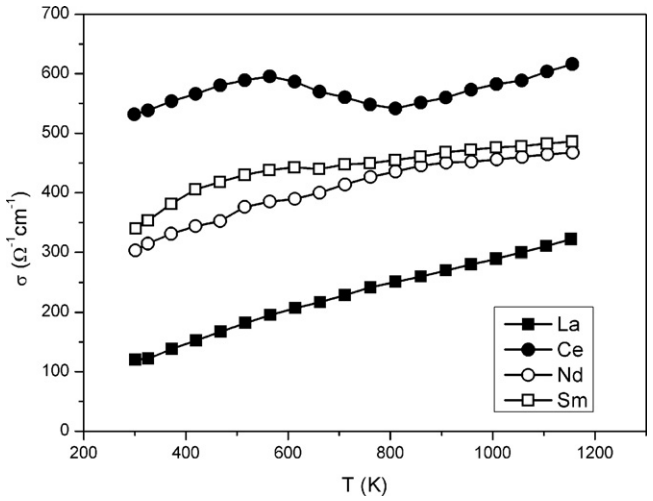

Fig. 2. Electrical conductivity of $LaMo_8O_{14}$, $CeMo_8O_{14}$, $NdMo_8O_{14}$ and $SmMo_8O_{14}$ pellets consolidated by spark plasma sintering.

sified conventional sintering method [17] as expected. This could be due to higher density of the pellets made from SPS, occurring with smaller amount of boundaries between grains, and/or the generation of oxygen deficiencies.

The dependence of the Seebeck coefficient on the temperature is shown in Fig. 3. The Seebeck coefficient of every sample is negative over the whole temperature range, showing that the majority of charge carriers are electrons. The Seebeck coefficient at room temperature is −37 μV/K for $LaMo_8O_{14}$, −49 μV/K for $CeMo_8O_{14}$, −18 μV/K for $NdMo_8O_{14}$, and −12 μV/K for $SmMo_8O_{14}$, which are too low for thermoelectric applications. With increasing temperature, the Seebeck coefficient values of both $NdMo_8O_{14}$ and $SmMo_8O_{14}$ increase until a maximum of −62 μV/K for $NdMo_8O_{14}$ at 1000 K and −34 μV/K for $SmMo_8O_{14}$ at 760 K. These values are lower than the previous reports [17] of conventional sintering method possibly due to the oxygen deficiency after the SPS process.

Fig. 4 shows the temperature dependence of power factor, $S^2\sigma$. Because of the trend of the decreasing Seebeck coefficient with increasing temperature for $LaMo_8O_{14}$ and $CeMo_8O_{14}$, the power factors decrease with increasing temperature for these two compounds. On the other hand, the power factors of the Nd

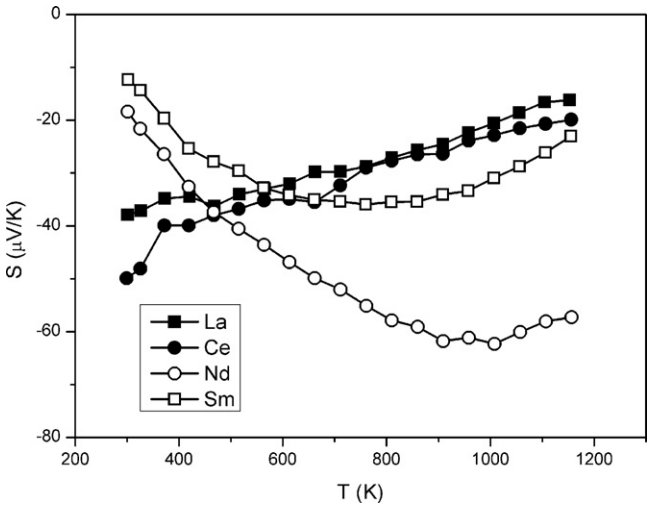

Fig. 3. Seebeck coefficient of $LaMo_8O_{14}$, $CeMo_8O_{14}$, $NdMo_8O_{14}$ and $SmMo_8O_{14}$ pellets consolidated by spark plasma sintering.

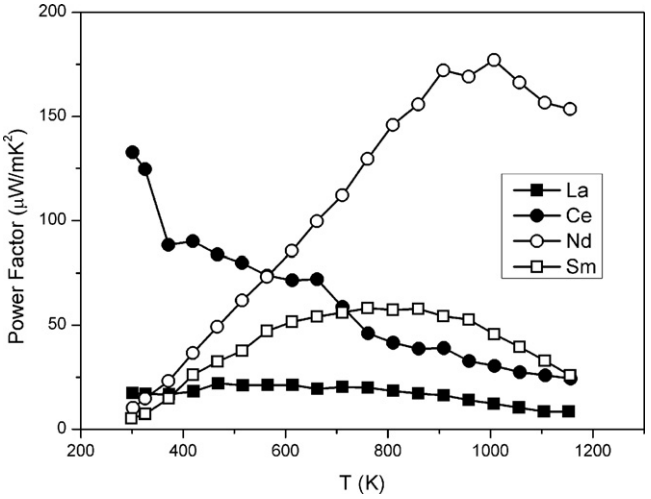

Fig. 4. Power factors of $LaMo_8O_{14}$, $CeMo_8O_{14}$, $NdMo_8O_{14}$ and $SmMo_8O_{14}$ pellets consolidated by spark plasma sintering.

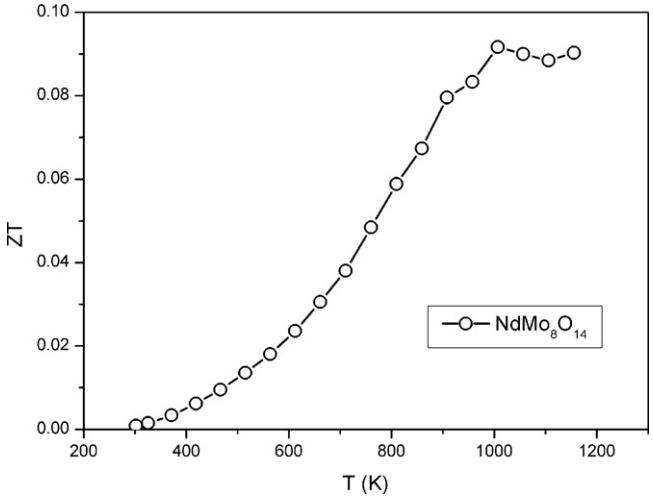

Fig. 6. The dimensionless figure of merit of a $NdMo_8O_{14}$ pellet consolidated by spark plasma sintering.

and Sm compounds increase with the increasing of the temperature, reaching maximum values of 177 μW/mK^2 at 1000 K and 58 μW/mK^2 at 760 K, respectively. The maximum power factor value for $NdMo_8O_{14}$ obtained from SPS is three times larger than that obtained from the conventional sintering method [17], and compares well with some state of arts n-type thermoelectric oxides like $CaMn_{0.98}Nb_{0.02}O_3$ [11], while it is still lower than in some p-type oxides such as $Ca_3Co_{3.95}Ga_{0.05}O_9$ [31].

In order to calculate the dimensionless figure of merit of ZT for $NdMo_8O_{14}$, thermal conductivity, κ, of $NdMo_8O_{14}$ was evaluated as shown in Fig. 5. The C_p we obtained from the ratio method at 323.15 K is about 0.7 J/g/K, comparable with the one estimated from the Dulong–Petit law [32], i.e., 0.5 J/g/K. The total thermal conductivity of $NdMo_8O_{14}$ was determined to be 3.19 W/mK at 322 K, which is comparable with some classic thermoelectric oxides [11,12,25]. The thermal conductivity value decreases with increasing temperature until 2.0 W/mK at 1164 K, which is favorable for the high temperature thermoelectric application. According to our knowledge, this constitutes the first report on thermal conductivity of a reduced molybdenum oxide with Mo clusters. The relatively low thermal conductivity is likely a consequence of the heavy lanthanide elements and the complex structure of $LnMo_8O_{14}$ [33–37].

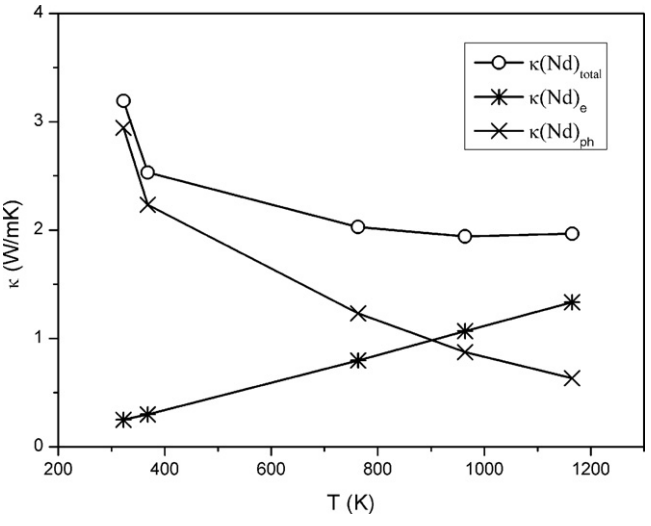

Fig. 5. The thermal conductivity of a $NdMo_8O_{14}$ pellet consolidated by spark plasma sintering.

The total thermal conductivity κ consists of the electronic contribution κ_e and the phonon contribution κ_{ph}, i.e. $\kappa = \kappa_e + \kappa_{ph}$. The electronic component can be estimated from the electrical conductivity by using the Wiedemann–Franz law, $\kappa_e = L_0\sigma T$, where $L_0 = 2.45 \times 10^{-8}$ WΩ/K^2 is the Lorenz number and T is the absolute temperature. The calculated κ_e and κ_{ph} are summarized in Fig. 5 as well. The main contribution to the total thermal conductivity is the phonon part around room temperature, and the electronic part is almost negligible. The electronic part starts to play an important role at high temperature because of the increasing number of charge carriers.

Using the measured electrical conductivity and Seebeck coefficient, and fitted thermal conductivity data, the dimensionless figure of merit, ZT, of $NdMo_8O_{14}$ was evaluated as shown in Fig. 6. The ZT value increases with the increasing of temperature, and the maximum values reach 0.1 at 1000 K, which is promising for thermoelectric application as a new n-type oxide system still needs to be optimized.

5. Conclusion

Thermoelectric properties of four molybdenum oxides, $LaMo_8O_{14}$, $CeMo_8O_{14}$, $NdMo_8O_{14}$ and $SmMo_8O_{14}$ made by SPS were examined. Comparing with the conventional sintering method, the thermoelectric performances of these oxides were improved by SPS. Among them, $NdMo_8O_{14}$ has the highest power factor at high temperature. $NdMo_8O_{14}$ also exhibits a low thermal conductivity from around room temperature up to 1164 K. The maximum ZT of 0.1 was obtained for this compound at 1000 K, which is within the same order of magnitude like that of current state-of-the art n-type thermoelectric oxides.

Acknowledgements

This work was supported by the Fuels Cells and Solid State Chemistry Division at Risø National Laboratory in Denmark.

References

[1] D.M. Rowe, CRC Handbook of Thermoelectrics, CRC Press, Boca Raton, FL, 1995.
[2] I. Terasaki, Y. Sasago, K. Uchinokura, Phys. Rev. B 56 (1997) 12685–12687.
[3] M. Hervieu, P. Boullay, C. Michel, A. Maignan, B. Raveau, J. Solid State Chem. 142 (1999) 305–382.
[4] A.C. Masset, C. Michel, A. Maignan, M. Hervieu, O. Toulemonde, F. Studer, B. Raveau, J. Hejtmanek, Phys. Rev. B 62 (2000) 166–175.

[5] M. Hervieu, A. Maignan, C. Michel, V. Hardy, N. Creon, B. Raveau, Phys. Rev. B 67 (2003) 045112–045119.
[6] R. Funahashi, I. Matsubara, H. Ikuta, T. Takeuchi, U. Mizutani, S. Sodeoka, Jpn. J. Appl. Phys. 39 (2000) 1127–1129.
[7] K. Kurosaki, T. Oyama, H. Muta, M. Uno, S. Yamanaka, J. Alloys Compd. 372 (2004) 65–69.
[8] Y. Cui, J.R. Salvador, J. Yang, H. Wang, G. Amow, H. Kleinke, J. Electron. Mater. 38 (2009) 1002–1007.
[9] S. Ohta, T. Nomura, H. Ohta, K. Koumoto, J. Appl. Phys. 97 (2005) 034106.
[10] S. Ohta, T. Nomura, H. Ohta, M. Hirano, H. Hosono, K. Koumoto, Appl. Phys. Lett. 87 (2005) 092108.
[11] L. Bocher, M.H. Aguirre, D. Logvinovich, A. Shkabko, R. Robert, M. Trottmann, A. Weidenkaff, Inorg. Chem. 47 (2008) 8077–8085.
[12] G. Xu, R. Funahashi, Q. Pu, B. Liu, R. Tao, G. Wang, Z. Ding, Solid State Ionics 171 (2004) 147–151.
[13] I. Matsubara, R. Funahashi, T. Takeuchi, S. Sodeoka, T. Shimizu, K. Ueno, Appl. Phys. Lett. 78 (2001) 3627–3629.
[14] W. Shin, N. Murayama, K. Ikeda, S. Sago, J. Power Sources 103 (2001) 80–85.
[15] L. Zhang, T. Tosho, N. Okinaka, T. Akiyama, Mater. Trans. 49 (2008) 1675–1680.
[16] M. Ohtaki, K. Araki, K. Yamamoto, J. Electron. Mater. 38 (2009) 1234–1238.
[17] J. Xu, M. Sonne, N. Pryds, H. Kleinke, J. Alloys Compd. 489 (2010) 353–356.
[18] S.J. Hibble, S.P. Cooper, A.C. Hanon, S. Patat, W.H. McCarroll, Inorg. Chem. 37 (1998) 6839–6846.
[19] J. Tortelier, P. Gougeon, R. Gautier, R. Berjoan, Inorg. Chem. 40 (2001) 2292–2297.
[20] C.C. Torardi, R.E. McCarley, J. Am. Chem. Soc. 101 (1979) 3963–3964.
[21] P. Gall, N. Barrier, R. Gautier, P. Gougeon, Inorg. Chem. 41 (2002) 2879–2885.
[22] J. Tortelier, P. Gall, H. Noel, P. Gougeon, J. Solid State Chem. 152 (2000) 403–411.
[23] J. Tortelier, P. Gougeon, Inorg. Chem. 37 (1998) 6229–6236.
[24] M. Tokita, J. Soc. Powder Technol. Japan 30 (1993) 790–804.
[25] I. Matsubara, R. Funahashi, K. Takahata, S. Sodeoka, J. Appl. Phys. 90 (2001) 462–465.
[26] C. Recknagel, N. Reinfried, P. Höhn, W. Schnelle, H. Rosner, Y. Grin, A. Leithe-Jasper, Sci. Technol. Adv. Mater. 8 (2007) 357–363.
[27] Q.M. Lu, J.X. Zhang, X. Zhang, Y.Q. Liu, D.M. Liu, M.L. Zhou, J. Appl. Phys. 98 (2005), 106107-106101-106107-106103.
[28] J.X. Zhang, Q.M. Lu, K.G. Liu, L. Zhang, M.L. Zhou, Mater. Lett. 58 (2004) 1981–1984.
[29] J.G. Noudem, M. Prevel, A. Veres, D. Chateigner, J. Galy, J. Electroceram. 22 (2009) 91–97.
[30] Y. Cui, J. He, G. Amow, H. Kleinke, Dalton Trans. 39 (2010) 1031–1035.
[31] N.V. Nong, C.J. Liu, M. Ohtaki, J. Alloys Compd. 491 (2010) 53–56.
[32] R.K. Fitzgerel, F.H. Verhoek, J. Chem. Educ. 37 (1960) 545.
[33] G. Kerihuel, J. Tortelier, P. Gougeon, Acta Crystallogr. C 52 (1996) 2389–2393.
[34] H. Leligny, P. Labbe, M. Ledesert, M. Hervieu, B. Raveau, W.H. McCarroll, Acta Crystallogr. B 49 (1993) 444–454.
[35] G. Kerihuel, P. Gougeon, Acta Crystallogr. C 51 (1995) 787–790.
[36] P. Gougeon, R.E. McCarley, Acta Crystallogr. C 47 (1991) 241–244.
[37] J. Tortelier, P. Gougeon, Acta Crystallogr. C 53 (1997) 668–671.